First-principles study of strain-induced modulation of energy gaps of graphene/BN and BN bilayers

Xiaoliang Zhong, Yoke Khin Yap, and Ravindra Pandey[*]

Department of Physics, Michigan Technological University, Houghton, Michigan, 49931, USA

Shashi P. Karna[†]

US Army Research Laboratory, Weapons and Materials Research Directorate, ATTN: RDRL-WM,
Aberdeen Proving Ground, Maryland 21005-5069, USA

First-principles calculations based on density functional theory are performed on graphene/BN and BN bilayers to investigate the effect of the strain on their energy gaps. For the graphene/BN bilayer, the bands have characteristic graphenelike features with a small band gap at K. Application of strain modulates the band gap, whose magnitude depends on the strength of interaction between constituent monolayers. For the BN bilayer, on the other hand, a large band gap is predicted, which remains nearly the same for small strains. The increased inhomogeneity in charge density of different carbon sublattices due to a stronger interplanar interaction is the cause of the predicted variation in the band gap with strains applied along the perpendicular direction in the graphene/BN bilayer.

PACS number(s): 73.22.Pr

I. INTRODUCTION

Graphene is a two-dimensional monoatomic layer system which has attracted great research interest due to its remarkable electronic properties.[1–3] Its honeycomb lattice can be described in terms of a sp^2 hybridized network of carbon atoms. In the reciprocal space of graphene, p_z bands cross at the Fermi level, and the absence of gap is related to the equivalence of the two carbon sublattices of graphene.[1] When the two sublattices are made inequivalent, a significant modification in electronic properties of the semimetallic graphene can be expected.

Hexagonal boron nitride (h-BN), with a similar lattice constant but different boron and nitrogen sublattices, is suggested to be a suitable choice as a substrate to introduce the inequivalence in the graphene lattice.[4] For example, a gap with a value of $\sim$0.053 eV was predicted for graphene deposited on a h-BN substrate.[4] The choice of an O-terminated SiO$_2$ substrate was reported to introduce a finite gap of $\sim$0.35 eV due to a strong covalent interaction between the monolayer and the substrate.[5] Likewise, experimental results based on angle-resolved photoemission spectroscopy[6] found a gap of $\sim$0.26 eV at the K point in epitaxial graphene on a SiC substrate. However, recent experiments[7] using the C face of SiC report well-defined Dirac cone dispersion at the K point. First-principles calculations,[8] on the other hand, predict a formation of a strong graphitic-substrate bond for graphene on a (0001) 4H-SiC surface. Furthermore, theoretical calculations based on a tight-binding model have investigated the influence of electric field on the band structure of a graphene/BN bilayer, predicting an increase in its energy gap.[9]

Considering that the presence of strain can also affect the electronic properties of a given system, we propose to investigate the effect of strain applied to a graphene/BN bilayer on its energy gap in the present study. We will also examine the role of interplanar interaction in determining the electronic properties of a bilayer system by comparing the results of graphene/BN with a BN bilayer system. Note that both theoretical and experimental studies have investigated the effect of intraplanar strain on the electronic properties of a graphene monolayer, reporting a shift of the Fermi crossing away from the high-symmetry k points.[10–12] The rest of the Brief Report is organized as follows: Sec. II gives the details of the computational method. Results are discussed in Sec. III, and a summary is given in Sec. IV.

II. COMPUTATIONAL METHOD

Total energy calculations were performed in the framework of the local density approximation of the exchange and correlation functional to density functional theory (LDA-DFT) as implemented in the SIESTA computational code.[13] We make use of Troullier-Martins pseudopotential[14] and double-ζ basis sets with polarization functions for all atoms. A vacuum distance of 15 Å between neighboring bilayer systems was used. The calculated equilibrium configurations associated with the graphene/BN and BN bilayers are fully relaxed, with residual forces smaller than 0.01 eV/Å. It should be pointed out that the LDA-DFT method has been shown to provide a reasonably good description of the physics and chemistry of graphitic or h-BN systems,[15–17] although it underestimates the band gap of the semiconducting and ionic materials. Nevertheless strain-modulated features in the band structure of the bilayers considered are clearly demonstrated by the LDA-DFT method employed here.

The graphene/BN bilayer consists of a stacking of one BN monolayer and one graphene monolayer, both of a sp^2-bonded hexagonal structure. Following the stacking nomenclature of graphite, we define the arrangements to be AA (i.e., C atoms are on top of either B or N atoms of the BN layer), AB (nitrogen) (i.e., one C atom is on top of a N atom and the other C atom is on top of the center of the hexagon of the BN layer), and AB (boron) (i.e., a C atom is on top of a B atom and the other C atom is on top of the center of the hexagon of the BN layer). Similarly, the stacking arrangements in a BN bilayer are AA (i.e., B$_I$ is positioned at top of B$_{II}$ and N$_I$ is positioned at top of N$_{II}$), AA' (i.e., B$_I$ is positioned at top of N$_{II}$ and N$_I$ is positioned at top of B$_{II}$), AB (boron) (i.e., B$_I$ is on top of B$_{II}$,
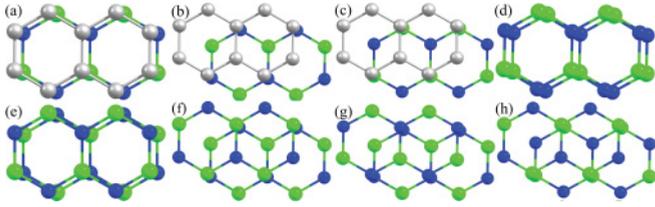
FIG. 1. (Color online) A schematic diagram of the stacking arrangements considered for graphene/BN and BN bilayers. The gray, green, and blue represent carbon, boron, and nitrogen atoms, respectively. Z is the interplanar separation of the system.

while N_I is on the center of hexagon of the second BN layer), AB (nitrogen) (i.e. ,N_I is on top of N_{II}, while B_I is on the center of hexagon of the second BN layer), and AB (i.e., B_I is on top of N_{II} and N_I is on top of the center of hexagon of the second BN layer). Here, the subscripts I and II refer to the atoms associated with first and second layers of BN, respectively. The stacking configurations considered for graphene/BN and BN bilayers are shown in Fig. 1.

III. RESULTS AND DISCUSSION

A. Structural properties

Figure 2 shows a representative calculated energy surface for the graphene/BN and BN bilayers, where a variation in the interplanar separation is used to represent the strain applied to the bilayer along the vertical direction.

The calculated structural parameters, namely, intraplanar bond length (i.e., near-neighbor distance R) and interplanar separation Z, together with the binding energy (E_B) of the graphene/BN and BN bilayers are given in Table I. E_B is defined as the total energy of a bilayer minus the sum of total energies of the corresponding constituent monolayers. We note that monolayers of BN have been fabricated with an aim to explore their potential applications in electronics.[18,19]

For the graphene/BN bilayer, the calculated results predict the AB (boron) stacking arrangement to be energetically preferred, although the energy difference between the AB (boron) and other two is relatively small (~ 0.01 eV/atom). In the equilibrium AB (boron) configuration, the interplanar spacing is 3.022 Å and the intraplanar bond length (for both R_{B-N} and R_{C-C}) is 1.429 Å. It is to be noted here that calculations find the AB stacking configuration ($R = 1.422$ Å, $Z = 3.022$ Å, $E_B = -0.24$ eV) to be energetically preferred
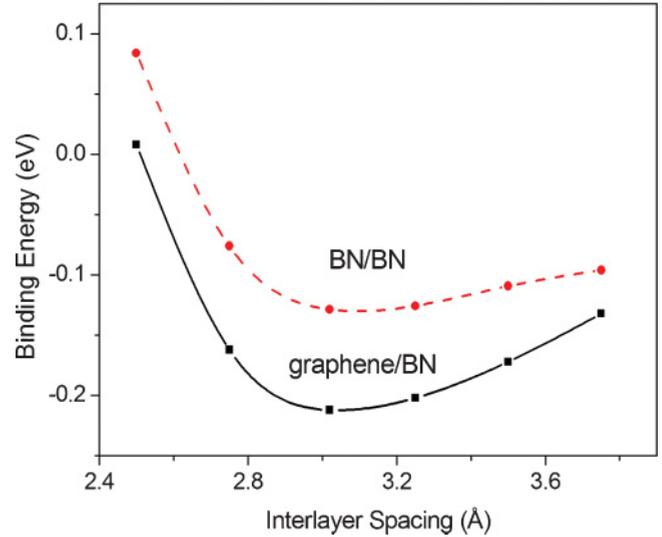

FIG. 2. (Color online) Binding energy (E_B) vs interlayer separation (Z) for graphene/BN and BN bilayers of the lowest-energy stacking patterns [(a) and (h) in Fig. 1].

over the AA configuration ($R = 1.423$ Å, $Z = 3.225$ Å, $E_B = -0.186$ eV) for the graphene bilayer system. Our results are in agreement with previous theoretical results obtained for graphene on the h-BN substrate, where the AB (boron) stacking arrangement was found to be preferred over the other two stacking arrangements at the LDA-DFT level of theory.[4]

For the BN bilayer, the AB stacking arrangement is predicted to be the optimal configuration, closely followed by the AA' and AB (boron) stacking arrangements. The calculated R_{B-N} remains nearly the same for all stacking arrangements, whereas the calculated interplanar separation does vary with the stacking arrangements. The calculated R_{B-N} of 1.44 Å for the BN bilayer is slightly different from the typical value of 1.42 Å in the sp^2 network of carbon atoms. Note that the calculated R_{B-N} of ~ 1.45 Å for the monolayer BN is in agreement with the results of previous theoretical studies.[20–24]

The AA' stacking configuration of the BN bilayer reflects the atomic arrangement of the bulk h-BN for which the experimental values of the lattice constants a and c are 2.505 and 6.662 Å, respectively.[25] In the AA' stacking configuration, the calculated values of a and c are 2.489 and 6.206 Å, respectively, indicating that a BN bilayer system may not be

TABLE I. Structural properties of the bilayer systems: graphene/BN and BN.

| System	Label	Stacking configuration	Binding energy (eV)	(Intraplanar) bond length R (Å)	Interplanar separation Z (Å)
Graphene/BN	Fig. 1(a)	AA	-0.168	1.427	3.208
Graphene/BN	Fig. 1(b)	AB (nitrogen)	-0.171	1.427	3.244
Graphene/BN	Fig. 1(c)	AB (boron)	-0.207	1.429	3.022
BN/BN	Fig. 1(d)	AA	-0.101	1.437	3.429
BN/BN	Fig. 1(e)	AA'	-0.129	1.437	3.103
BN/BN	Fig. 1(f)	AB	-0.133	1.438	3.071
BN/BN	Fig. 1(g)	AB (nitrogen)	-0.099	1.438	3.357
BN/BN	Fig. 1(h)	AB (boron)	-0.128	1.438	3.065
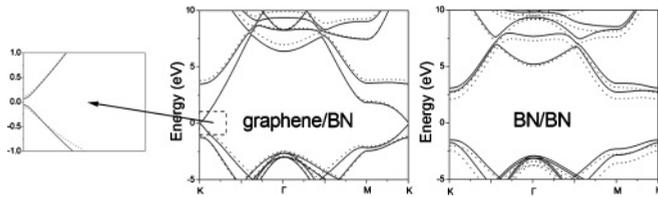
FIG. 3. Band structure of the equilibrium (solid lines) and strained (dotted lines) configuration of graphene/BN and BN bilayers. The left-hand panel shows the band structure near the K point.
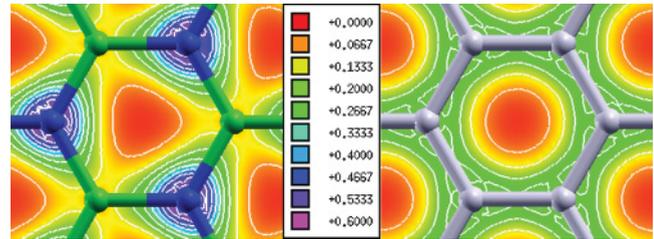

FIG. 4. (Color online) The valence-band charge-density contours of BN (left-hand side) and graphene (right-hand side) of the graphene/BN bilayer. The central panel shows the scale of charge density, in units of e^-/Bohr^3.

appropriate to simulate the structural properties of the bulk h-BN.

B. Electronic structure

Band structures of the energetically preferred stacking arrangements for graphene/BN and BN bilayers [i.e., AB (boron) and AB for graphene/BN and BN bilayer, respectively] along the high symmetry points in k space are shown in Fig. 3. In the graphene/BN bilayer, we find that the bands near the Fermi level have characteristic graphenelike features with linear dispersion. The degeneracy of bands at the so-called Dirac points K and K' appears to be lifted, leading to an energy gap of $\sim$0.12 eV. This is in contrast to the case of the BN bilayer, where a direct energy gap of $\sim$4.3 eV at K in the k space is predicted. For the crystalline h-BN, the LDA-DFT level of theory finds a minimum indirect gap of 4.02 eV, which increases to 5.95 eV after incorporating the GW quasiparticle corrections.[26,27] Interestingly, experimental measurements have suggested the minimum gap to be direct, with a value of 5.97 eV.[28]

Our calculations, therefore, predict a large opening of the gap for an isolated bilayer graphene/BN system relative to that predicted for a graphene deposited on the h-BN bulk substrate.[4] Note that the substrate was simulated by four h-BN layers[4] with an optimum interlayer distance of 3.22 Å between the graphene and the substrate. In our work, the calculated interlayer distance is 3.24 Å when we use four layers to simulate BN.

The opening of energy gap in graphene/BN can be attributed to the interplanar interaction between graphene and BN monolayers. Carbon atoms in graphene appear to experience a slightly different electrostatic potential due to an inhomogeneous charge distribution present in BN, thus making them to be inequivalent.[1] This is confirmed by the valence-band charge-density plots of the constituent BN and graphene monolayers (Fig. 4). The valence-band charge-density contours of the BN monolayer consists of a pattern of a curved triangle, reflecting the different electronegativity of boron and nitrogen. Indeed, the charge density around nitrogen is approximately three times that around boron. In contrast, the charge contours of the graphene monolayer reveal near similarity of two carbon sublattices. On the other hand, the neutral pristine graphene bilayer bulk is gapless,[29] while a gap can be opened if the symmetry of the two carbon monolayers is broken, e.g., in the presence of a transverse electric field.[30]

A large energy gap predicted for the BN bilayer is due to the partial ionic character of the chemical bond between boron and nitrogen in the lattice. In the equilibrium configuration, the interplanar interaction appears to slightly reduce the energy gap of the BN bilayer relative to that calculated ($\sim$4.5 eV) for the BN monolayer.

C. Strain-modulated band structure

In the following, we restrict ourselves to investigate the effect of small strains ($\leqslant$10%) on the band structure, considering that small strains are not likely to lead to significant distortions in the atomic arrangements in the constituent monolayers. For example, the monolayer BN is found to be slightly buckled in graphene/BN; the difference in the Z coordinate (i.e., c axis perpendicular to the plane) of B and N is $\sim$0.008 Å, with B moving toward the graphene. The simulated pressure is perpendicular to the intraplanar C-C bonds, and the magnitude of the strain was simulated by varying the interplanar separation Z in graphene/BN and BN bilayers.

Figure 5 shows the variation of the band gap at K with the strain for the graphene/BN and BN bilayers. The nature of the strain-modulated gap at K in k space for graphene/BN is significantly different from that exhibited by the BN bilayer.

For the graphene/BN bilayer, the strain increases the strength of the interaction between the constituent monolayers which, in turn, increases the energy gap at K. For the small strains considered, the relationship is predicted to be linear; the gap is $\sim$0.2 eV for $\sim$9% strain applied along the c axis.
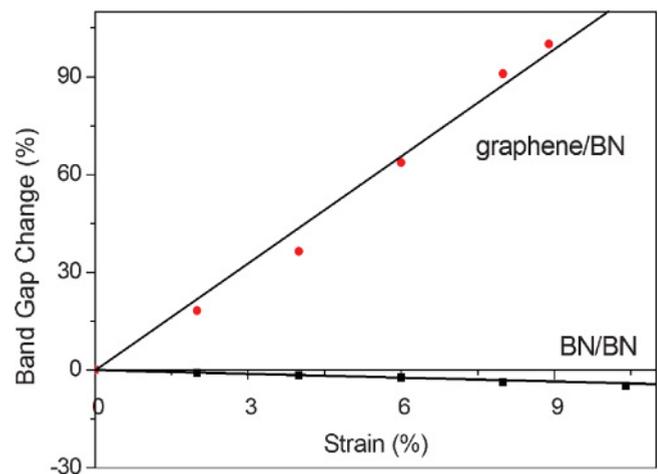

FIG. 5. (Color online) Variation of the band gap with the strain perpendicular to the graphene/BN and BN bilayers.

At the equilibrium configuration of graphene/BN, the upper valence band is dominated by C-p_z orbitals, leading to linear dispersion of the π band near the Fermi level. A higher degree of interplanar interaction leads to somewhat flattening of the bands near the Fermi level, which can be attributed to the change in the nature of the upper valence band. Note that the projected density of states of graphene/BN (not shown here) finds an increased contribution from N-p_z orbitals in forming the upper valence band with an increase in the strain.

The calculated results do not show such a drastic variation in the band gap of the BN bilayer with an increase in the strain; the band gap at K is slightly decreased for $\sim$10% strain relative to that for the equilibrium configuration. For the BN bilayer, the upper valence band is composed of N-p_z orbitals whereas the lower conduction band is dominated by B-p_z orbitals. Their positions with respect to the Fermi level remain nearly the same in k space for the small strains considered. Note that our calculated values of the c-axis compressibility in units of (10^{-12} cm^2/dyn) are 2.92 and 3.31 for graphene/BN and BN bilayers, respectively, as compared to the experimental value of 2.44 (10^{-12} cm^2/dyn) for the c-axis compressibility of the graphite crystal at 0 K.[31]

IV. SUMMARY

The LDA-DFT level of theory predicts the equilibrium configurations of graphene/BN and BN bilayers to be *AB* (boron) and *AB* stacking configurations, respectively. The calculated band gaps are 0.12 and 4.3 eV, respectively, for graphene/BN and BN bilayers in their energetically preferred equilibrium configurations. The strain-induced modulation of the band gap is investigated by varying the interplanar separation of the constituent monolayers. The magnitude of the band gap appears to be directly related to the strain applied perpendicular to the graphene/BN bilayer. On the other hand, the band gap of the BN bilayer remains nearly the same for the small strains considered. The increased inhomogeneity of different carbon sublattices due to a stronger interplanar interaction is the cause of larger band gaps at the higher strains applied for the graphene/BN bilayer.

*pandey@mtu.edu

†shashi.karna@us.army.mil

[1] A. H. Castro Neto, F. Guinea, N. M. R. Peres, K. S. Novoselov, and A. K. Geim, Rev. Mod. Phys. **81**, 109 (2009).

[2] A. K. Geim and K. S. Novoselov, Nat. Mater. **6**, 183 (2007).

[3] M. I. Katsnelson, Mater. Today **10**, 20 (2007).

[4] G. Giovannetti, P. A. Khomyakov, G. Brocks, P. J. Kelly, and J. van den Brink, Phys. Rev. B **76**, 073103 (2007).

[5] P. Shemella and S. K. Nayak, Appl. Phys. Lett. **94**, 032101 (2009).

[6] S. Y. Zhou, G. H. Gweon, A. V. Fedorov, P. N. First, W. A. de Heer, D. H. Lee, F. Guinea, A. H. Castro Neto, and A. Lanzara, Nat. Mater. **6**, 770 (2007).

[7] E. Moreau, S. Godey, F. J. Ferrer, D. Vignaud, X. Wallart, J. Avila, M. C. Asensio, F. Bournel, and J.-J. Gallet Appl. Phys. Lett. **97**, 241907 (2010).

[8] F. Varchon, R. Feng, J. Hass, X. Li, B. N. Nguyen, C. Naud, P. Mallet, J. Y. Veuillen, C. Berger, E. H. Conrad, and L. Magaud, Phys. Rev. Lett. **99**, 126805 (2007).

[9] J. Slawinska, I. Zasada, and Z. Klusek, Phys. Rev. B **81**, 155433 (2010).

[10] M. Mohr, K. Papagelis, J. Maultzsch, and C. Thomsen, Phys. Rev. B **80**, 205410 (2009).

[11] G. Gui, J. Li, and J. Zhong, Phys. Rev. B **78**, 075435 (2008).

[12] M. Huang, H. Yan, C. Chen, D. Song, T. F. Heinz, and J. Hone, Proc. Natl. Acad. Sci. USA **106**, 7304 (2009).

[13] D. SanchezPortal, P. Ordejon, E. Artacho, and J. M. Soler, Int. J. Quantum Chem. **65**, 453 (1997).

[14] N. Troullier and J. L. Martins, Phys. Rev. B **43**, 1993 (1991).

[15] S. B. Trickey, F. Müller-Plathe, G. H. F. Diercksen, and J. C. Boettger, Phys. Rev. B **45**, 4460 (1992).

[16] A. Marini, P. García González, and A. Rubio, Phys. Rev. Lett. **96**, 136404 (2006).

[17] N. Ooi, A. Rairkar, and J. B. Adams, Carbon **44**, 231 (2006).

[18] K. S. Novoselov, A. K. Geim, S. V. Morozov, D. Jiang, M. I. Katsnelson, I. V. Grigorieva, S. V. Dubonos, and A. A. Firsov, Nature (London) **438**, 197 (2005).

[19] J. Kotakoski, C. H. Jin, O. Lehtinen, K. Suenaga, and A. V. Krasheninnikov, Phys. Rev. B **82**, 113404 (2010).

[20] J. Li, G. Gui, and J. Zhong, J. Appl. Phys. **104**, 094311 (2008).

[21] F. W. Averill, J. R. Morris, and V. R. Cooper, Phys. Rev. B **80**, 195411 (2009).

[22] M. Topsakal, E. Aktürk, and S. Ciraci, Phys. Rev. B **79**, 115442 (2009).

[23] S. Azevedo, J. R. Kaschny, Caio M. C. de Castilho, and F de Brito Mota, Nanotechnology **18**, 495707 (2007).

[24] S. Azevedo, J. R. Kaschny, C. M. C. de Castilho, and F. D. Mota, Eur. Phys. J. B **67**, 507 (2009).

[25] R. S. Pease, Acta Crystallogr. **5**, 356 (1952).

[26] B. Arnaud, S. Lebègue, P. Rabiller, and M. Alouani, Phys. Rev. Lett. **96**, 026402 (2006); B. Arnaud, S. Lebègue, P. Rabiller, and M. Alouani, **100**, 189702 (2008)

[27] L. Wirtz, A. Marini, M. Grüning, C. Attaccalite, G. Kresse, and A. Rubio, Phys. Rev. Lett. **100**, 189701 (2008).

[28] K. Watanabe, T. Taniguchi, and H. Kanda, Nat. Mater. **3**, 404 (2004).

[29] E. McCann and V. I. Fal'ko, Phys. Rev. Lett. **96**, 086805 (2006).

[30] T. Ohta, A. Bostwick, T. Seyller, K. Horn and E. Rotenberg, Science **313**, 951 (2006).

[31] W. B. Gauster and I. J. Fritz, J. Appl. Phys. **45**, 3309 (1974).